Molecular Crystals and Liquid Crystals

Publication details, including instructions for authors and subscription information:
http://www.tandfonline.com/loi/gmcl20

Change of Order of Nematic Phase Transition in Uniaxially Anchored Systems

Muniriding Yasen [a], Masashi Torikai [a] & Mamoru Yamashita [a]

[a] Department of Physics Engineering, Mie University, Kamihama, Tsu, Japan

Version of record first published: 31 Aug 2006

To cite this article: Muniriding Yasen, Masashi Torikai & Mamoru Yamashita (2005): Change of Order of Nematic Phase Transition in Uniaxially Anchored Systems, Molecular Crystals and Liquid Crystals, 438:1, 77/[1641]-90/[1654]

To link to this article: http://dx.doi.org/10.1080/15421400590954434

Mol. Cryst. Liq. Cryst., Vol. 438, pp. 77/[1641]–90/[1654], 2005

ISSN: 1542-1406 print/1563-5287 online
DOI: 10.1080/15421400590954434

Change of Order of Nematic Phase Transition in Uniaxially Anchored Systems

Muniriding Yasen
Masashi Torikai
Mamoru Yamashita
Department of Physics Engineering, Mie University, Kamihama, Tsu, Japan

Nematic phase transition with both uniaxial and biaxial order parameters is studied in the two kind of external fields where are conjugate to the order parameters, respectively. A global phase diagram on the fields versus temperature space is obtained in the mean field theory, which is similar topologically to the phase diagram of the three-state Potts in three dimension. From this phase diagram, the phase diagram of the system in the uniaxial field is derived, and the result is applied to the phase transition of the thin system anchored uniaxially, i.e., by the homeotropic and planer walls.

Keywords: biaxial ordering; effective field; global phase diagram; Maier-Saupe model; nematic phase; uniaxial cell

INTRODUCTION

Liquid crystals are characterised by an orientational order, and the ordering behaviour is well-described, at least qualitatively, by the Maier-Saupe model [1–3]. Though this model is rather simple, various phase changes are known theoretically to occur in this model, corresponding to varieties of experimental facts. An ordering direction of a nematic phase is degenerate and the continuous symmetry is broken by an external field. In the magnetic (or, electric) field, the first order transition occurring at the weak field strength changes to a critical behaviour at a certain critical field strength and no transition occurs at high field for the system with positive paramagnetic (or, dielectric) anisotropy [4–7].

Address correspondence to Muniriding Yasen, Department of Physics Engineering, Mie University, Kamihama 1515, Tsu, 514–8507, Japan. E-mail: munirdin@qe.phen.mie-u.ac.jp

A boundary wall is also an agency to break the symmetry of the orientatianal order. The effect of the boundary walls to enhance the nematic order is discussed theoretically by Sheng in the framework of Landau theory [8], where the first order transition disappears at the system with thickness smaller than a certain critical thickness. This phenomenon is certified experimentally by Yokoyama [9]. The change of phase transition at thin system anchored by the walls resembles to the one at the system in the field above mentioned [4–7], showing a similarity of the effects due to the external field and boundary. In the practical application to liquid crystal displays, the competition between both effects due to the field and boundaries [10] is utilised. However, the difference between them should be also noted. After these investigations, various theoretical and experimental studies about the ordering behaviour at various confined systems have been carried out [11–13]. In the study of a smectic layer ordering at the system anchored homeotropically, one of the present author and his coworker have introduced a method to study the transition of thin system, in which an inhomogeneity due to the boundaries is expressed in terms of an effective field which depends not only on temperature but on position [14]. The behaviour of the system is argued by observing a locus of the effective field on the phase diagram of field versus temperature plane.

This theory has been applied to various problems, the nematic ordering [15–17], the smectic one [18] and a phase transition of a freely suspended film of ferroelectric smentics [19,20]. The phase diagram of the bulk plays an important role in the theory, and a derivation of the phase diagram in the external field is inevitable. In the previous study of nematics [16], phase transitions in a uniaxial field with a tricritical point (which is first pointed out by Fan and Stephen [21]) together with a critical point is studied, where a similarity of the global phase diagram to the one at the tree-state Potts model in three dimension [22–24] is suggested. On the basis of this phase diagram, phase transitions under various types of anchored conditions are classified systematically [16]. In the present paper, we study minutely the phase transitions occurring at the Maier-Saupe model exposed to the two kinds of external fields which are conjugated to a uniaxial and biaxial order parameters, respectively, and apply the results to the phase transitions of thin systems.

In the next section, two order parameters and conjugated fields are introduced, and general formalism for the Maier-Saupe model is given in the mean field theory. Following to this, the global phase diagram is obtained by the numerical analysis. A certain cross section of global phase diagram is nothing but the phase diagram in the uniaxial field

[16,21], based on which the phase change in the thin system anchored uxiaxially is discussed. Finally, summary is given.

GENERAL FORMALISM–MAIER-SAUPE MODEL

The nematic order parameter s is usually given as a thermal average by

$$s = \frac{1}{N_t}\sum_{i}^{N_t}\langle P_2(\cos\theta_i)\rangle, \tag{1}$$

where θ is an angle between a long axis of i-molecule and a preferred direction along which the orientational order will appear, $P_2(x)\,(=(3x^2-1)/2)$ the second Legendre's polynomial and N_t denotes the total number of molecules. Corresponding to s, the symmetry breaking field h is introduced, and the field energy H_{ext} is expressed as

$$H_{ext} = -h\sum_{i} P_2(\cos\theta_i). \tag{2}$$

In case the magnetic field H is applied, h is equal to $\chi_a H^2/2$ with χ_a the anisotropic part of paramagnetic susceptibility. Though h is true symmetry breaking field for the case of positive anisotropy, another order parameter and symmetry breaking field are required for the negative anisotropy, because the long range order should appear in the plane perpendicular to h.

Let h be in direction to z-axis. Generally, all directions are equivalent, and we introduce here $P_2(\cos v_{ix})$, $P_2(\cos v_{iy})$ and $P_2(\cos v_{iz})$ with direction cosines $\cos v_{ix}$, $\cos v_{iy}$ and $\cos v_{iz}$ ($v_{iz} = \theta_i$), and conjugate field h_x, h_y and h_z. Then, the field energy H_{ext} is generalised as

$$H_{ext} = -\sum_{i}\{h_x P_2(\cos v_{ix}) + h_y(\cos v_{iy}) + h_z(\cos v_{iz})\}. \tag{3}$$

For those, $P_2(\cos v_{ix})$, $P_2(\cos v_{iy})$ and $P_2(\cos v_{iz})$ the following identity satisfied,

$$P_2(\cos v_{ix}) + P_2(\cos v_{iy}) + P_2(\cos v_{iz}) = 0. \tag{4}$$

We see that independent parameters are two and that a quantity $\{P_2(\cos v_{ix}) - P_2(\cos v_{iy})\}$ describes the broken symmetry in the x-y plane. We introduce here another order parameter σ given by [16,21]

$$\begin{aligned}\sigma &= \frac{2}{3}\frac{1}{N_t}\sum_{i}\langle P_2(\cos v_{ix}) - P_2(\cos v_{iy})\rangle \\ &= \frac{1}{N_t}\sum_{i}\langle \sin^2\theta_i \cos 2\varphi_i\rangle,\end{aligned} \tag{5}$$

in which φ_i denotes the azimuthal angle of i-th molecule. As two variables are independent, independent conjugate fields are also two, and we can choose h_y arbitrarily with no loss of generality. By choosing h_y to be $-h_x$ and using h' $(= 3/2h_x)$, H_{ext} is reduced to

$$H_{\text{ext}} = -\sum_i \{h' \sin^2 \theta_i \cos 2\varphi_i + h_z P_2(\cos \theta_i)\}, \tag{6}$$

In the mean field theory, the Maier-Saupe Hamiltonian is given by [1–3,16]

$$H_0 = -V \sum_{(i,j)} P_2(\cos \theta_{i,j}) \tag{7}$$

where θ_{ij} denotes an angle between long axis of i-th and j-th molecules and V an effective coupling constant.

The partition function in the symmetry breaking field $\eta(= \beta h')$ and $\zeta(= \beta h_z)$ is written as

$$Z(\eta, \zeta) = \prod_i \Big[\int_0^{2\pi} d\varphi_i \int_0^{\pi} d\theta_i \sin \theta_i \exp\{\eta \sin^2 \theta_i \cos 2\varphi_i + \zeta P_2(\cos \theta_i)\}\Big] e^{-\beta H_0}, \tag{8}$$

in which β is the inverse temperature $1/k_{\text{B}}$ with Boltzmann constant k_{B}. It is well known that the result derived from the partition function obtained up to the order β equivalent to the one in the mean field theory [15,16]. We write $Z(\eta, \zeta)$ in an expansion form as

$$Z(\eta, \zeta) = \prod_i \Big[\int_0^{2\pi} d\varphi_i \int_0^{\pi} d\theta_i \sin \theta_i \exp\{\eta \sin^2 \theta_i \cos 2\varphi_i + \zeta P_2(\cos \theta_i)\}\Big] \times \big((1 - \beta H_0) + O(\beta^2)\big). \tag{9}$$

A partition function for one molecule is defined by

$$z(\eta, \zeta) = \int_0^{2\pi} d\varphi_i \int_0^{\pi} d\theta_i \sin \theta_i \exp\big\{\eta \sin^2 \theta_i \cos 2\varphi_i + \zeta P_2(\cos \theta_i)\big\} \tag{10}$$

and function $I(\eta,\zeta)$ and $J(\eta,\zeta)$ are introduce as,

$$I(\eta, \zeta) = \frac{\partial \ln z(\eta, \zeta)}{\partial \eta}, \tag{11}$$

$$J(\eta, \zeta) = \frac{\partial \ln z(\eta, \zeta)}{\partial \zeta}. \tag{12}$$

Then, partition function (9) is calculate as

$$Z(\eta,\zeta) = z^{N_t}(\eta,\zeta)\left[1 + \frac{N_t \beta V z}{2}\left(\frac{3}{4}I^2 + J^2\right) + O(\beta^2)\right], \tag{13}$$

in which z denotes a mean number of the nearest neighoiring molecules for one molecule and we use an addition theorem for $P_2(\cos\theta_{ij})$ given by

$$P_2(\cos\theta_{ij}) = P_2(\cos\theta_i)P_2(\cos\theta_j) + \frac{3}{4}\sin 2\theta_i \sin 2\theta_j \cos(\varphi_i - \varphi_j) + \frac{3}{4}\sin^2\theta_i \sin^2\theta_j \cos 2(\varphi_i - \varphi_j). \tag{14}$$

It is noticed that the second term in Eq. (14) has no contribution to $Z(\eta,\zeta)$. Because Eq. (13) is calculated up to the order β, we obtain the following expression,

$$\ln Z(\eta,\zeta) = N_t\left\{\ln z(\eta,\zeta) + \frac{\beta V z}{2}\left(\frac{3}{4}I^2 + J^2\right)\right\}. \tag{15}$$

The order parameter σ and s are given by

$$\sigma = \frac{1}{N_t}\frac{\partial \ln Z(\eta,\zeta)}{\partial \eta} = I(\eta,\zeta) + \beta V z\left\{\frac{3}{4}I(\eta,\zeta)\frac{\partial I(\eta,\zeta)}{\partial \eta} + J(\eta,\zeta)\frac{\partial J(\eta,\zeta)}{\partial \eta}\right\}. \tag{16}$$

$$s = \frac{1}{N_t}\frac{\partial \ln Z(\eta,\zeta)}{\partial \zeta} = J(\eta,\zeta) + \beta V z\left\{\frac{3}{4}I(\eta,\zeta)\frac{\partial I}{\partial \zeta} + J(\eta,\zeta)\frac{\partial J(\eta,\zeta)}{\partial \zeta}\right\}. \tag{17}$$

Taking account of the relation, $\partial I(\eta,\zeta)/\partial\zeta = \partial J(\eta,\zeta)/\partial\eta$ $(= \partial^2 \ln z(\eta,\zeta)/\partial\eta\partial\zeta)$, Eqs. (16) and (17) are reduced to the following forms up to the order β as,

$$\sigma = I\left(\eta + \frac{3}{4}\beta V z\sigma, \zeta + \beta V z s\right), \tag{18}$$

$$s = J\left(\eta + \frac{3}{4}\beta V z\sigma, \zeta + \beta V z s\right). \tag{19}$$

Those Eqs. (18) and (19) are the self-consistency equations, which will be solved numerically in the following section.

The free energy ΔF is calculated as a function of σ and s by

$$\beta\Delta F = \int_0^s ds'\zeta(0,s') + \int_0^\sigma d\sigma'\eta(\sigma',s), \tag{20}$$

where $\eta(\sigma, s)$ and $\zeta(\sigma, s)$ are determined from Eqs. (18) and (19). By using eqs. (18) and (19) we can rewrite ΔF in the form as,

$$\Delta F = \frac{1}{2}Vz\left(\frac{3}{4}\sigma^2 + s^2\right) - k_B T \ln\frac{z\left(\frac{3}{4}\beta Vz\sigma + \beta h', \beta Vzs + \beta h_z\right)}{z(0,0)}. \tag{21}$$

GLOBAL PHASE DIAGRAM

Here, numerical analyses of the self-consistency Eqs. (18) and (19) are carried out in the fields h' and h_z, that is, $h_x = 2/3h'$ and $h_y = -h_x$. It is noticed that the case, $h_z = h_x = -h_y$ $(=h_0)$, is identical to the fields, $h_z = h_x = 0$, $h_y = -2h_0$. Because of the equivalence of the three fields, h_z, h_x and h_y, we have only to study the case, $h_z \geq h_x \geq 0$. In Figure 1, the coexisting curve which ends at the critical point C is shown for various values of h_x; (a) 0, (b) 0.005, (c) 0.10, (d) 0.015 and (e) 0.02 (here and hereafter, the fields are scaled in the unit Vz and the temperature in Vz/k_B). The tricritical point labelled as TCP is located at $T_t = 0.2415$ and $h_{xt} = 0.02692$ [16]. From those results, the critical

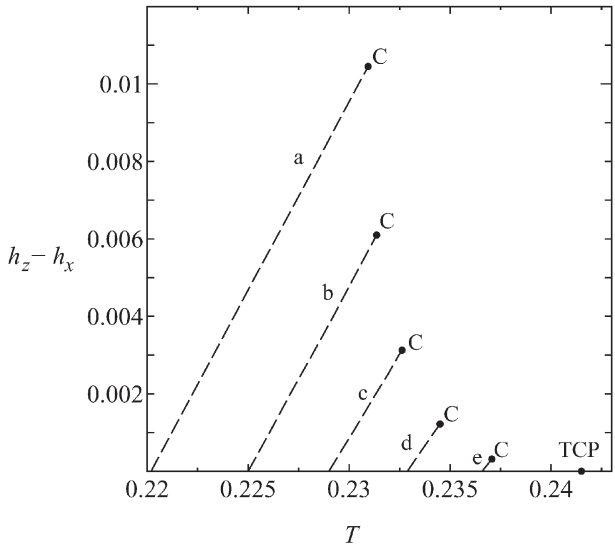

FIGURE 1 Coexisting curve, where $h_y = -h_x$ and values of h_x are; (a) 0, (b) 0.005, (c) 0.01, (d) 0.015 and (c) 0.02 in the unit Vz.

curve is obtained in the h_z versus h_x plane as shown in Figure 2, where the critical curve for $h_x > h_{xt}$ is located on the line $h_z = h_x$. The area between the critical curve C-TCP and the dotted thin line ($h_z = h_x$) indicates the coexisting surface, whose cross sections are the coexisting curves in Figure 1. Near TCP the critical curve has the form as $h_z - h_x = \mathrm{a}(h_{xt} - h_x)^{\alpha}$ with an estimate $\alpha \cong 2.7$ as shown in Figure 3, in which three lines with slopes 2, 2.7, 3, respectively, are drawn for a guide of eye.

The set of values of the fields (h_x, $-h_x$, h_z) in the above study is identical to the set ($2h_x$, 0, $h_x + h_z$). Taking account of the identity, the phase diagram on the h_z versus h_x plane under the condition $h_y = 0$ is derived by mapping Figure 2 on this plane, which is mapped successively onto the h_x–h_y–h_z plane with oblique coordinate system as shown in Figure 4, where we use the equivalence of three fields and symmetry of reflection. It is stressed that the oblique coordinate system is essential in the present system, because the horizontal direction, ($h_x - h_y$) with the strength $h_x = h_y$, and the vertical one, h_z, correspond to the symmetry breaking fields h' and h, respectively. This phase diagram is similar topologically to the one for three-state Potts model in three dimension [22–24]. In the previous study, this

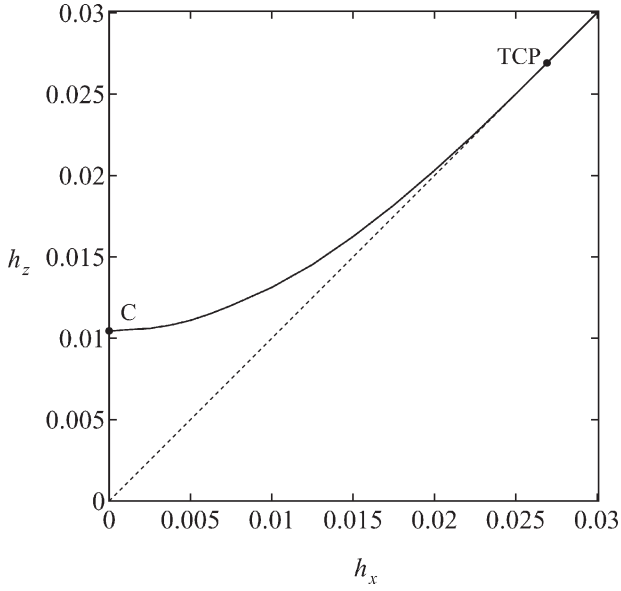

FIGURE 2 Critical curve in the h_z versus h_x plane the condition $h_y = -h_x$, where TCP denotes the tricritical point.

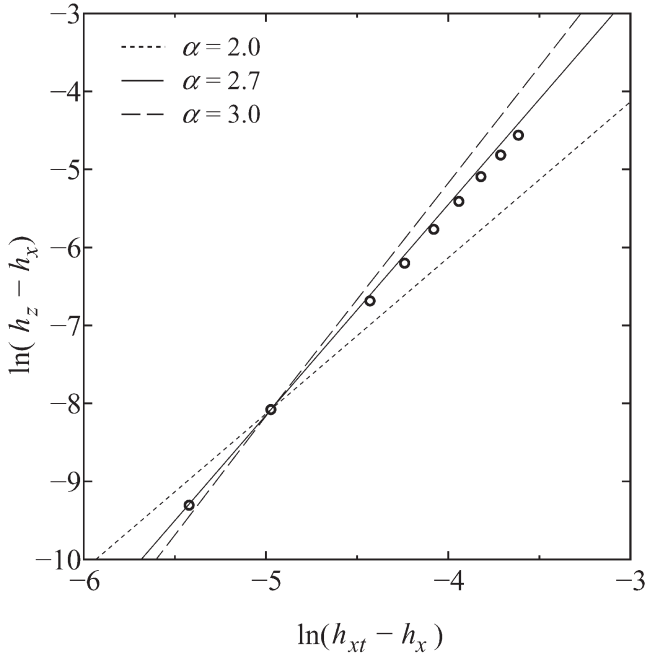

FIGURE 3 Plot of the critical curve of figure 2 near TCP where $\ln(h_z - h_x)$ versus $\ln(h_{xt} - h_x)$ are plotted showing the index 3.

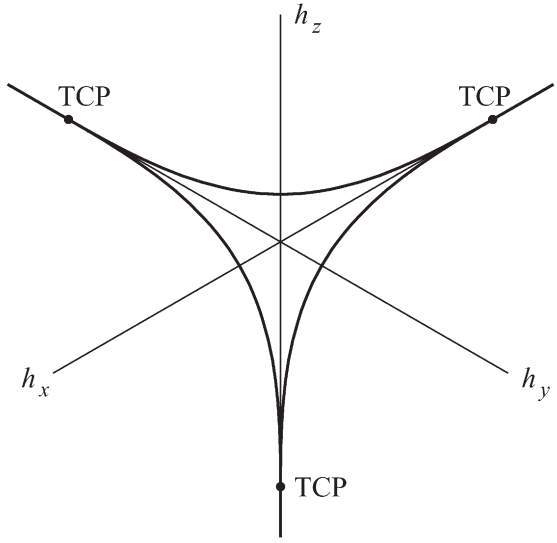

FIGURE 4 Phase diagram on the oblique $h_x - h_y - h_z$ plane.

types of phase diagram is suggested from the argument based on the symmetry consideration combined with the location of the critical point one [16]. Here, the phase diagram, especially the detail of critical curve, is certified by the concrete numerical calculation.

UNIAXIALLY ANCHORED PHASES

Phase Transition in the Uniaxial Field

For the purpose of discussing the phase transition off the system anchored uniaxially, we obtain the phase diagram in the uniaxial field, which is nothing but the cross section of Figure 4 at a certain axis, say, z-axis. In Figure 5, the phase diagram is shown in which the broken curves denote the coexisting curves and the solid one the critical line. The coexisting curve in the positive field region indicates the coexistence of two phases, high temperature phase and the ordered one in the z-direction, while the curve in the negative field region is the triple line along which three phases, ordered phase in the x-, and y-directions, respectively, together with the high temperature phase, coexist. We have another triple line lying on the T-axis, where three ordered phases coexist. We notice here the magnitude of tricritical value $|h_t|$ ($= 0.05383$) in this plane is twice of h_{xt} in Figure 2. Temperature dependences of the order parameters describing the

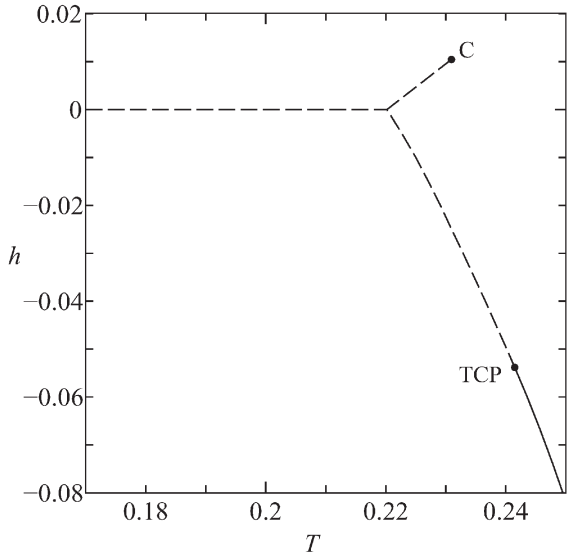

FIGURE 5 Phase diagram in the uniaxial field h.

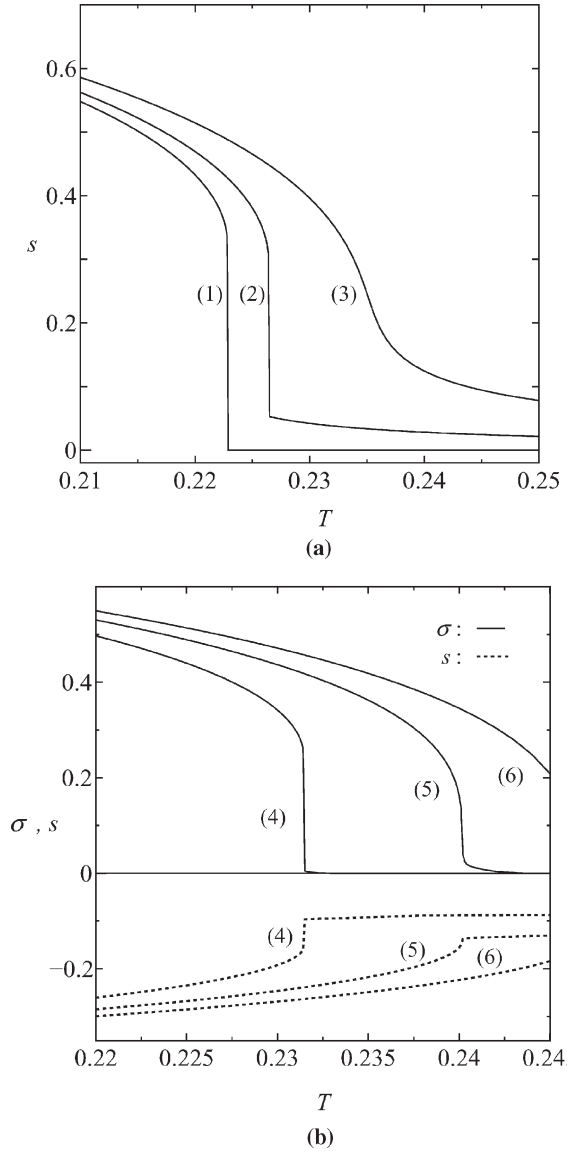

FIGURE 6 Temperature dependences of s and σ for various value of h.

behaviour of the system are shown in Figure 6 for several values of h; (1) +0, (2) 0.005, (3) 0.015 in (a) and (4) −0.025, (5) −0.05, (6) −0.07 in (b). For positive value of the field σ vanishes irrespective of temperature.

Change of Ordering Process in the Thin System Anchored Uniaxially

In the inhomogeneous system anchored by the walls, the order parameters changes depending on the position ρ denoting the distance from the boundary wall; $\sigma(\rho)$ and $s(\rho)$. The molecular field applied to $P(\cos\theta_i)$ of the i-th molecule at ρ is considered to be $V\{(z-2)s(\rho)+s(\rho+l)+s(\rho-l)\}$ on an average, where l denotes a mean separation of neighbouring molecules in the z-direction. So as to make the numerical study easy, we use the discretised expressions σ_n and s_n, $(n=1,2,\ldots,N)$, which corresponds to the treatment that the system is decomposed into N thin sheets with thickness l. Then, the molecular filed is expressed as $V\{(z-2)s_n+s_{n+1}+s_{n-1}\}$, which is rewritten in the form, (Vzs_n+h_n), with an effective field h_n defined by

$$h_n = V(s_{n+1}+s_{n-1}-2s_n) \tag{22}$$

Similarly, an effective field $h'n$ is defined by

$$h'_n = \frac{3}{4}V(\sigma_{n+1}+\sigma_{n-1}-2\sigma_n) \tag{23}$$

Here, we obtain the self-consistency equations for σ_{n} and s_n as [14,16,17]

$$\sigma_n = I\left(\beta h'_n+\frac{3}{4}\beta Vz\sigma_n, \beta h_n+\beta Vzs_n\right), \tag{24}$$

$$s_n = J\left(\beta h'_n+\frac{3}{4}\beta Vz\sigma_n, \beta h_n+\beta Vzs_n\right). \tag{25}$$

These forms are same to the bulk ones under the effective fields $h'n$ and h_n. In case the fields are constant, the behaviour of σ_n and s_n are same to the bulk ones (18) and (19). The Eqs. (24) and (25) suggest the similarity and also the difference between both effects due to the fields and anchoring walls, whereas $h'n$ and h_n are dependent of temperature and position.

The homeotropic anchoring system has been studied detail; at a certain thickness of the system, the first order phase transition changes to the critical behaviour, and for the system of thichness smaller than that no phase transition occurs [8,17]. The profile of is concave and the effective field h_n given by Eq. (22) is positive, while σ_n and h_n are zero. By observing h_n on the positive field area of Figure 5, it has been found that near this critical thickness unstable state which never appears at the bulk system occurs in the inner portion of the system [17]. The appearance of such unstable state in the thin

system shows the typical difference of the effect caused by the walls from that due to the external field.

To see what happens at the planer anchoring system, we show in Figure 7 the phase diagram in h' versus T plane for representative two cases; (a) $|h| < |h_t|$ and (b) $|h| > |h_t|$, which are the cross sections of Figure 4 and 5 with constant h_z values larger and smaller than h_t, respectively. The coexisting curves appearing in the finite field region of h' in (a) come from Figure 1.

For the planer system with enough thickness, the first order transition is assumed to occur, in which the high temperature phase is uniaxial with quite small but negative value of s_n induced by the anchoring walls. The profile of $\{s_n\}$ is convex and accordingly h_n takes negative value, while σ_n and h'_n are zero because no symmetry is broken in the xy-plane. The negativeness of h_n above mentioned is common to the low temperature phase, in which the ordering is biaxial because the symmetry is broken. Irrespective of the profile of $\{\sigma_n\}$, convex or concave, h'_n jumps from zero to a finite value at the transition point. The general feature of h'_n is sketched by the dotted curve in (a) of Figure 7. As the thickness becomes small, the magnitude of h_n increases. If $|h_n|$ exceeds the tricriical value at sufficiently small thickness, the phase diagram (a) should be replaced by (b), and the behaviour of h'_n becomes such a curve shown schematically by dotted curve in (b), where no jump of the order parameter is observed. In contrast with the case of homeotropic anchoring walls where the first order transition changes to no transition as the thickness becomes small, the transition changes to the second order one at the system with planer walls.

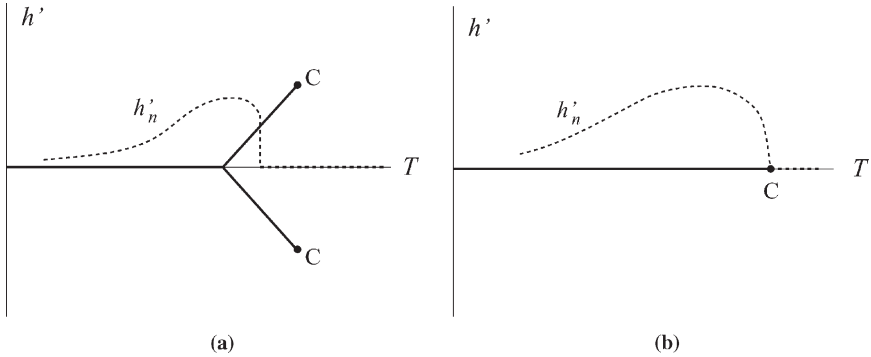

FIGURE 7 Phase diagram in h' versus T plane where (a) $h < h_t$ and (b) $h > h_t$. The broken thin curve indicates the supposed behaviour of h'_n.

SUMMARY

The global phase diagram of the nematic ordering is obtained in the two kinds of fields corresponding to the uniaxial and biaxial order parameters. Taking into account the symmetry of the order parameter space, the phase diagram in the field space with oblique three-fold axes is derived, which is similar topologically to the one for the three-state Potts model in three dimension. Two kind of critical lines cross tangentially with the index about 2.7 at the critical point. These results are applied to ordering phenomenon in the system with planer anchoring walls, where the first order phase transition changes to the second order one as the thickness of the system becomes small. Though this behaviour has been already suggested, we can discuss this problem on the concrete ground obtained in this study.

Previously, Fan and Stephen pointed out the change of order of phase transition under the uniaxial field by phenomenological argument, in which the tricritical point is derived on the basis of free energy of expansion form in a couple of order parameter at the region, the is, $(s, \sigma) = (0, 0)$ [21]. The correct derivation of the tricritical point has been shown by one of the present authors, where the expansion is carried out at the tricritical point, $(s, \sigma) = (s_t, 0)$ with s_t the tricritical value of s [16].

In the course of the change from the first order phase transition to no transition via the critical behaviour as the thickness becomes small, the unstable state which never occurs in the bulk appears near the critical thickness in the homeotropically anchored nematic system [17] and freely suspended film of ferroelectric smectics [19,20]. In this context, it is quite interesting what happens near the crossover point from the first order transition to the second order one. To elucidate this problem, the practical study of the simultaneous Eq. (24) and (25) is required, and the results will be reported in the near future.

REFERENCES

[1] Maier, W. & Saupe, A. (1958). *Z. Naturforsch.*, *13a*, 564.
[2] Maier, W. & Saupe, A. (1959). *Z. Naturforsch.*, *14a*, 882.
[3] Maier, W. & Saupe, A. (1960). *Z. Naturforsch.*, *15a*, 287.
[4] Hanus, J. (1969). *Phys. Rev.*, *178*, 420.
[5] Wojtowicz, P. J. & Sheng, P. (1974). *Phys. Lett.*, *A48*, 235.
[6] Nicastro, A. J. & Keyes, P. H. (1984). *Phys. Rev.*, *A30*, 3156.
[7] Lelidis, I. & Durand, G. (1994). *Phys. Rev. Lett.*, *73*, 672.
[8] Sheng, P. (1976). *Phys. Rev. Lett.*, *37*, 1059.
[9] Yokoyama, H. (1988). *J. Chem. Soc. Faraday Trans.*, *84*, 1023.
[10] de Gennes, P. G. & Prost, J. (1993). *The Physics of Liquid Crystals*, Chapter 3, Clarendon Press: Oxford.

[11] Sluckin, T. J. & Poniewierski, A. (1990). *Mol. Cryst. Liq. Cryst.*, *179*, 349.
[12] Wittebrood, M. M., Luijendijk, D. H., Stallinga, S., Rasing, Th., & Musevic, I. (1996). *Phys. Rev.*, *E54*, 5232.
[13] van Effenterre, D., Ober, R., Valignat, M. P., & Cazabat, A. M. (2001). *Phys. Rev. Lett.*, *87*, 125701.
[14] Yamashita, M. & Miyazaki, T. (2001). *J. Phys. Soc. Jpn.*, *70*, 1611.
[15] Yamashita, M. (2003). *Mol. Cryst. Liq. Cryst.*, *398*, 75.
[16] Yamashita, M. (2003). *J. Phys. Soc. Jpn.*, *72*, 1682.
[17] Yasen, M., Torikai, M., & Yamashita, M., (2004). *J. Phys. Soc. Jpn.*, *73*, 2453.
[18] Torikai, M. & Yamashita, M., (2004). *J. Phys. Soc. Jpn.*, *73*, 2154.
[19] Yamashita, M. (2003). *J. Phys. Soc. Jpn.*, *72*, 2421.
[20] Yamashita, M. preprint submitted to *Ferroelectrics*.
[21] Fan, C. & Stephen, J. (1970). *M. Phys. Rev. Lett.*, *25*, 500.
[22] Straley, J. P. & Fisher, M. E. (1973). *J. Phys.*, *A6*, 1310.
[23] Yamashita, M. (1979). *Prog. Theor. Phys.*, *61*, 1287.
[24] Wu, F. Y. (1982). *Rev. Mod. Phys.*, *54*, 235.